

## Material parameters for thermoelectric performance

M N TRIPATHI<sup>1,2</sup> and C M BHANDARI<sup>3</sup>

<sup>1</sup>Department of Physics, University of Allahabad, Allahabad 211 002, India

<sup>2</sup>C.M.P. Degree College, Allahabad, India

<sup>3</sup>Indian Institute of Information Technology, Allahabad 211 002, India

E-mail: ommadhav27@rediffmail.com; cmbhandari@yahoo.com

MS received 18 October 2004; revised 3 April 2005; accepted 13 April 2005

**Abstract.** The thermoelectric performance of a thermoelement is ideally defined in terms of the so-called figure-of-merit  $Z = \alpha^2\sigma/\lambda$ , where  $\alpha$ ,  $\sigma$  and  $\lambda$  refer respectively to the Seebeck coefficient, electrical conductivity and thermal conductivity of the thermoelement material. However, there are other parameters which are fairly good indicators of a material's thermoelectric 'worth'. A simple yet useful performance indicator is possible with only two parameters – energy gap and lattice thermal conductivity. This indicator can outline all potentially useful thermoelectric materials. Thermal conductivity in place of lattice thermal conductivity can provide some additional information about the temperature range of operation. Yet another performance indicator may be based on the slope of  $\alpha$  vs.  $\ln\sigma$  plots.  $\alpha$  plotted against  $\ln\sigma$  shows a linear relationship in a simplified model, but shows a variation with temperature and carrier concentration. Assuming that such a relationship is true for a narrow range of temperature and carrier concentration, one can calculate the slope  $m$  of  $\alpha$  vs.  $\ln\sigma$  plots against temperature and carrier concentrations. A comparison between the variation of  $ZT$  and slope  $m$  suggests that such plots may be useful to identify potential thermoelectric materials.

**Keywords.** Semiconductors; thermoelectric materials; figure-of-merit.

**PACS No.** 72.20.Pa

### 1. Introduction

A thermoelectric generator works between two different temperatures, and is somewhat like a heat engine, converting heat into electrical energy. The conversion efficiency of the device (ratio of electrical power generated to the heat absorbed at the hot junction) can be expressed in terms of the Carnot efficiency and the specific material parameter corresponding to the thermoelement. This material parameter, referred to as thermoelectric figure-of-merit ( $Z$ ), is of central interest in thermoelectric material research and is defined as [1–4]

$$Z = \frac{\alpha^2\sigma}{\lambda}, \quad (1)$$

where,  $\alpha$  is the Seebeck coefficient, and  $\sigma$  and  $\lambda$  refer to the electrical and thermal conductivity of the thermoelement material, respectively.

The figure-of-merit ( $Z$ ) provides a guideline to find out potentially good thermoelectric materials; it is convenient to define dimensionless figure-of-merit ( $ZT$ ), where  $T$  is the mean temperature. For a simplified theoretical model based on parabolic energy bands and single spherical valley,  $ZT$  may be written as [1–5]

$$ZT = \frac{\left(\left(s + \frac{5}{2}\right) - \xi\right)^2}{\left(s + \frac{5}{2}\right) + (\beta \exp(\xi))^{-1}}, \quad (2)$$

where,  $\beta$  is defined as

$$\beta = 5.74 * 10^{-6} T^{3/2} \left(\frac{m^*}{m_0}\right)^{3/2} \frac{\mu}{\lambda_L},$$

where  $\xi$  and  $s$  refer to reduced Fermi energy  $E_F/k_B T$  and scattering parameter, and  $m^*$ ,  $m_0$ ,  $\mu$ ,  $\lambda_L$ ,  $k_B$  refer to effective mass, free electron mass, carrier mobility, lattice thermal conductivity and Boltzmann constant, respectively.  $\beta$  has also been employed as an indicator for thermoelectric performance of materials. In a rigorous theoretical calculation  $Z$  takes a fairly complex form reflecting the features pertaining to several equivalent valleys, possible intra- and inter-valley scattering of carriers, non-parabolic nature of electron (hole) energy bands, and a likely contribution of the minority carriers. Whereas a final deciding factor reflecting on the merit and worth of the material is an exact calculation of  $Z$ , other indicators can present interesting and valuable guidelines too. We present in this paper two alternative methods for identifying materials for thermoelectric applications. (a) A preliminary guide, (b) slope of  $\alpha$  vs.  $\ln \sigma$  plot as an alternative performance indicator.

## 2. Theory

### (a) *A preliminary guide*

A material's usefulness in thermoelectric applications is displayed by a single entity referred to as the figure-of-merit which itself is a complex function of several physical parameters. Over the decades following the mid-twentieth century several material parameters were considered. The present paper suggests one of the simplest parameters that could be used as a preliminary guide to a material's usefulness in thermoelectric applications.

The three best-known groups of thermoelectric materials are those based on bismuth telluride, lead telluride and silicon–germanium alloys, and all these have widely differing values of figure-of-merit. Bismuth telluride-type materials have their highest value of  $Z$  around room temperature while silicon–germanium alloys have their highest value at about 1300 K. In the intermediate temperature range (400–800 K) materials based on lead telluride are among the best. However, when expressed in its dimensionless form the figure-of-merit  $ZT$  approximately approaches a value of unity for all three families of materials. The dimensionless

Material parameters for thermoelectric performance

**Table 1.** Room temperature values of energy gap, lattice thermal conductivity and  $\delta$  of thermoelectric materials.

Materials	Energy gap (eV)	Lattice thermal conductivity (W m <sup>-1</sup> K <sup>-1</sup> )	$\delta$ ((eV) <sup>1/2</sup> /W m <sup>-1</sup> )
GaSb	0.67	27	0.101
Bi <sub>2</sub> Te <sub>3</sub>	0.15	1.6	0.81
Sb <sub>2</sub> Te <sub>3</sub>	0.30	2.4	0.76
PbTe	0.32	2.0	0.94
PbSe	0.25	1.7	0.98
CdTe	1.50	7.5	0.54
InAs	0.35	29	0.068
InSb	0.17	15	0.092
ZnSb	0.6	17	0.16
InP	1.25	80	0.047
Ge	0.65	63	0.043
Si	1.15	113	0.032
Si-Ge <sup>1</sup>	0.97	7.6	0.432
Si-Ge <sup>2</sup>	0.97	3.3	0.99
Mg <sub>2</sub> Ge	0.60	13	0.20
Mg <sub>2</sub> Si	0.70	10.5	0.26
Mg <sub>2</sub> Sn	0.30	16	0.114
AgPb <sub>18</sub> SbTe <sub>20</sub>	0.30	1.99	0.92
GaAs	1.42	37	0.107

<sup>1</sup>Si<sub>70</sub>Ge<sub>30</sub> alloy single crystal; <sup>2</sup>fine grained material ( $\sim 5 \mu\text{m}$ ).

figure-of-merit thus represents a unifying quantity in the assessment of thermoelectric materials.

However, when attempting to identify potentially good thermoelectric materials, the required information on all the three parameters  $\alpha$ ,  $\sigma$  and  $\lambda$  is not always available in the literature. A simpler ratio, which appears to serve as an initial guide to good thermoelectric materials, is  $\sqrt{E_g}/\lambda_L$  where  $E_g$  is the energy gap. Expressing  $\lambda_L$  in W/m K and  $E_g$  in electron volts (eV), the ratio acquires an almost identical value for Bi<sub>2</sub>Te<sub>3</sub>, PbTe and SiGe alloys. Assuming that the lattice thermal conductivity varies as  $T^{-1}$  at room and higher temperatures and neglecting the temperature variation of  $E_g$  a better choice could be that a parameter,  $\delta = (\sqrt{E_g}/\lambda_L T) \times 10^3$ , can be defined, which is almost independent of temperature. Moreover for the best thermoelectric materials  $\delta$  approaches unity from below and gives a reasonably good agreement with the maximum value of  $ZT$  for these materials. Table 1 gives values of  $E_g$ ,  $\lambda_L$  and  $\delta$  for a large number of semiconductors [6–9]. Figure 1 displays  $\delta$  plotted against  $E_g$  for various materials. Larger values of  $\delta$  approaching unity are typically those of high-performance materials.

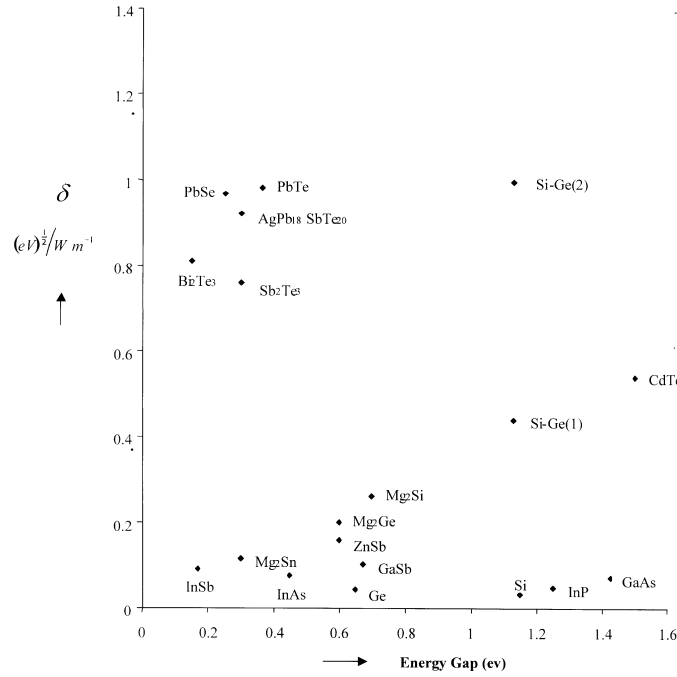


**Figure 1.** New material parameter  $\delta$  plotted against energy gap for different semiconductors.

(b) *Slope of  $\alpha$  vs.  $\ln \sigma$  plots as an alternative performance indicator*

For a simple theoretical model assuming parabolic energy bands and single spherical valley a simple relationship between the Seebeck coefficient and electrical conductivity can be given by [10,11]

$$\alpha = m(b - \ln \sigma), \tag{3}$$

where  $m = k_B/e$  and  $b \approx s + \ln[T^{3/2}(m^*/m_0)^{3/2}\mu] - 4.66$ .  $m$  and  $mb$  represent the slope and intercept on the  $\alpha$  vs.  $\ln \sigma$  plots.

It is investigated that maximum electrical power factor is dependent on both  $m$  and  $b$ . The use of  $\alpha$  vs.  $\ln \sigma$  plot only requires data from relatively simple measurements of  $\alpha$  and  $\sigma$  rather than  $m^*$  and  $\mu$ , which may be required to obtain  $ZT$  in accordance with eq. (2).

The non-parabolicity of energy bands has a considerable influence on the magnitude and variation of  $m$ , which is likely to be quite significant in narrow band-gap semiconductors [12]. The energy dependence of the effective mass is then given by [13,14]

$$m^* = m_0^*(1 + 2\beta_g\eta), \tag{4}$$

where  $\beta_g = k_B T/E_g$  and  $\eta = E/k_B T$ .

$E$  and  $E_g$  refer to carrier energy and energy band gap. The transport coefficients can be expressed in terms of generalized Fermi integrals, which are defined as [13–16]

$${}^n L_l^p(\xi, \beta_g) = \int_0^\infty \left( -\frac{\partial f}{\partial \eta} \right) \eta^n [\eta(1 + \beta_g \eta)]^p (1 + 2\beta_g \eta)^l d\eta. \quad (5)$$

Here  $f$  is the Fermi distribution function. The indices  $l, p, n$  take different values for various scattering processes.

The corresponding electron relaxation time for acoustic phonon scattering [13,15], which takes account of non-parabolicity of energy bands, is given by

$$\tau_{ac}^{-1} \propto [\eta(1 + \beta_g \eta)]^{1/2} [1 + 2\beta_g \eta]. \quad (6)$$

The reduced electrical conductivity  $\sigma'$  is given by

$$\sigma' = \left( \frac{k_B}{e} \right)^2 \frac{T}{\lambda_l} \sigma = K N_v {}^0 L_{-2}^1 \frac{T}{[m_c^* \lambda_l]}, \quad (7)$$

where  $N_v$  is the number of equivalent valleys and  $m_c^*$  is the conductivity effective mass. In the present calculations no distinction has been made between the density-of-states and conductivity effective masses. The constant  $K$  depends on the elastic constant  $C_{11}$  and acoustic deformation potential ( $\xi_D$ ) and is given by [4,8]

$$K = \frac{k_B^2 h C_{11}}{3\pi^2 \xi_D^2}. \quad (8)$$

In the two-band conduction model the electrical conductivity is the sum of contributions from both electrons and hole bands. Total Seebeck coefficient [14,16,17] is given by

$$\alpha = [\alpha_e \sigma_e + \alpha_h \sigma_h] / (\sigma_e + \sigma_h), \quad (9)$$

where, the contribution to the Seebeck coefficient from  $j$ th band can be expressed as

$$\alpha_j = \frac{k_B}{e} \left[ \frac{{}^1 L_{-2}^1}{{}^0 L_{-2}^1} - \xi_j \right]. \quad (10)$$

The total thermal conductivity [7,8] is then given as

$$\lambda = \lambda_L + \lambda_e + \lambda_h + \lambda_b, \quad (11)$$

where, suffices L, e, h and b refer to lattice, electron, hole and electron–hole pair (bipolar) contributions, respectively.

The electronic contribution to thermal conductivity is given by

$$\lambda_e = K N_v {}^0 L_{-2}^1 \frac{T}{m_c^*} \left( \frac{{}^2 L_{-2}^1}{{}^0 L_{-2}^1} - \left[ \frac{{}^1 L_{-2}^1}{{}^0 L_{-2}^1} \right]^2 \right). \quad (12)$$

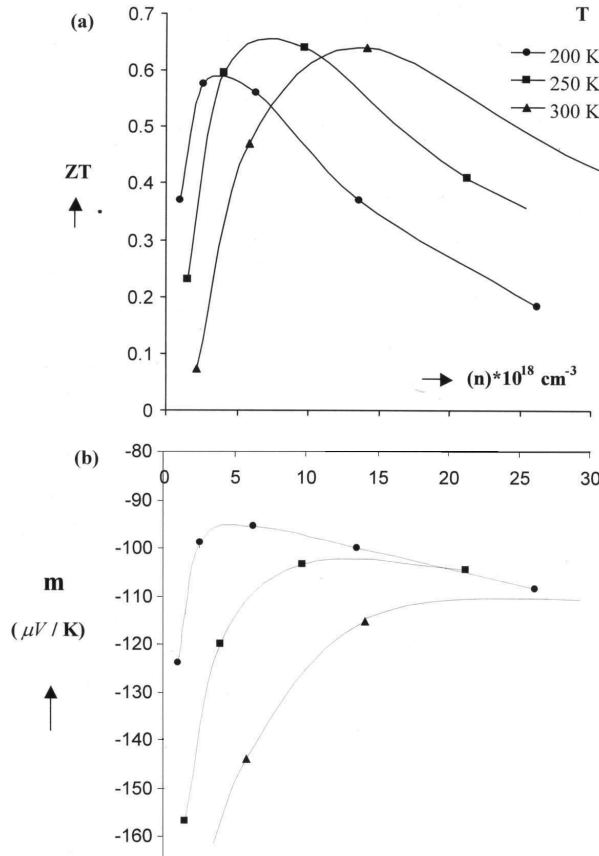


**Figure 2.** (a) Variation of figure-of-merit ( $ZT$ ) and (b) the value of slope  $m$  with carrier density ( $n$ ) at temperatures 200, 250 and 300 K for  $\text{Bi}_2\text{Te}_3$ .

The lattice thermal conductivity is given by [8,14]

$$\lambda_L = \left(\frac{k_B}{\hbar}\right)^3 \frac{k_B}{2\pi^2 v_s} T^3 \int_0^{\theta_D/T} \frac{x^4 e^x}{(e^x - 1)^2} \tau_C dx. \quad (13)$$

Here  $\theta_D$  is the Debye temperature.

For two-band conduction including bipolar contribution to thermal conductivity, the figure-of-merit [14,16–18] becomes

$$ZT = \frac{(\alpha'_h \sigma'_h - \alpha'_e \sigma'_e)^2}{\{(\sigma'_e + \sigma'_h)(1 + \sigma'_e L_e + \sigma'_h L_h) + \sigma'_e \sigma'_h (\delta_e + \delta_h + \xi_g)^2\}}, \quad (14)$$

where  $\delta = {}^1L_{-2}^1/{}^0L_{-2}^1$  and  $\xi_g = E_g/k_B T$ .

In the present paper we have presented the variation of the slope  $m$  and dimensionless figure-of-merit ( $ZT$ ) with respect to carrier concentration ( $n$ ). The three systems investigated, bismuth telluride ( $\text{Bi}_2\text{Te}_3$ ), lead telluride ( $\text{PbTe}$ ) and

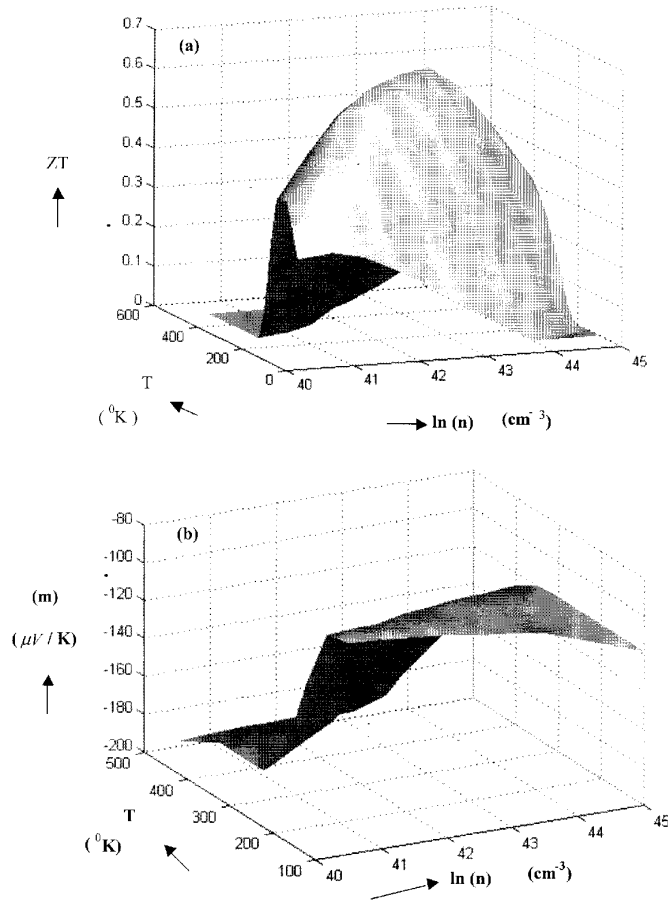


**Figure 3.** (a) 3D visualization of  $(ZT)$  and (b)  $m$  with log of carrier density  $(n)$  and temperature for  $\text{Bi}_2\text{Te}_3$  at the operating temperature range.

silicon–germanium alloys, are among the best-known thermoelectric materials for low, medium and higher temperature ranges.  $\text{Si}_{0.7}\text{Ge}_{0.3}$  is the best alloy composition among other compositions of silicon–germanium [14]. A linear interpolation is applied for physical parameters of  $\text{Si}_{0.7}\text{Ge}_{0.3}$ , except for  $\lambda_L$  which requires an independent calculation based on disorder scattering.

### 3. Results and discussion

Calculated values of  $\delta$  for a number of typical semiconductors are presented in table 1 and plotted in figure 1. Although only a limited number of semiconductor materials have been examined, there does appear to be a correlation between the parameter  $\delta$  and thermoelectric performance. It is concluded that in situations where insufficient information is available to evaluate the figure-of-merit, the

parameter  $\delta$  can serve as a useful indicator of the material's thermoelectric potential. It may be a sort of preliminary guide for probable candidates for thermoelectric applications.  $\delta$  can tell us about the usefulness of the material in the corresponding range of temperatures. It can also provide an indication of the optimum temperature range. Replacing  $\lambda_L$  by  $\lambda$  in the expression of  $\delta$  may provide an idea of optimum temperature range.  $\lambda_L T$  remains temperature independent, but  $\lambda T$  may increase with temperature in the intrinsic range and this may reduce the value of  $\sqrt{E_g}/\lambda_L T$ . This requires a detailed calculation of  $\lambda$  and will form the subject matter of a future work. Sofo and Mahan [19] found that the energy gap of high performance thermoelectric materials can be expressed by  $n k_B T$ , where  $n = 6-10$  and  $T$  is the operating temperature of thermoelectric device.

Referring to the second approach, eq. (3) suggests that a plot between  $\alpha$  vs.  $\ln \sigma$  is a straight line. This may be reasonably so in a narrow range of temperature and carrier density (reduced Fermi energy). However,  $m$  changes with both the

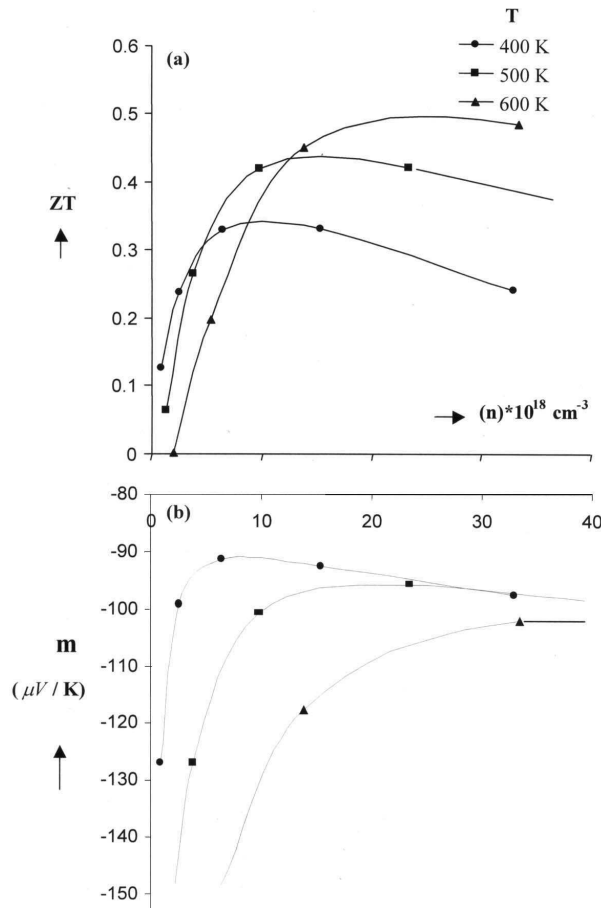


**Figure 4.** (a) Variation of figure-of-merit ( $ZT$ ) and (b) the value of slope  $m$  with carrier density ( $n$ ) in the temperature range (400–600 K) for PbTe.

Material parameters for thermoelectric performance

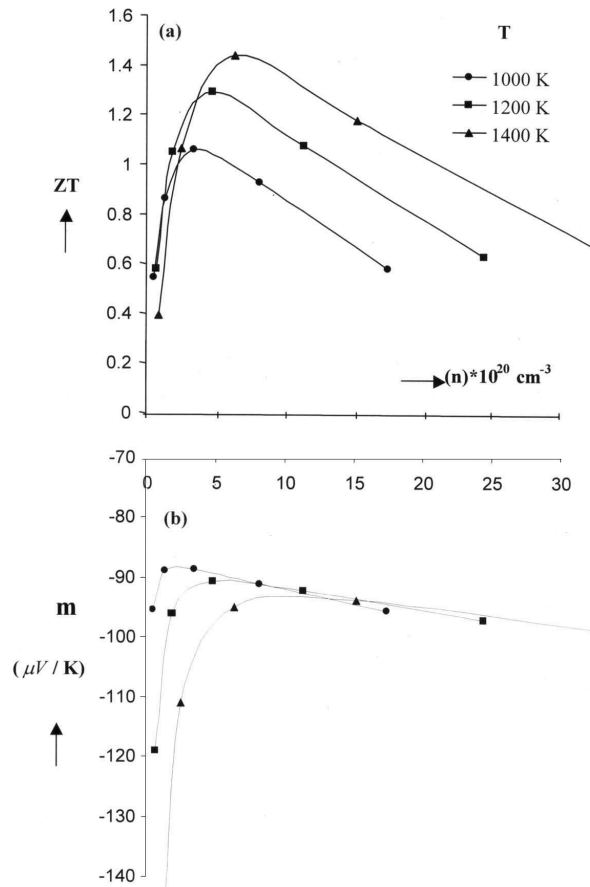


**Figure 5.** (a) Variation of figure-of-merit ( $ZT$ ) and (b) the value of slope  $m$  with carrier density ( $n$ ) at temperatures 1000, 1200 and 1400 K for  $\text{Si}_{0.7}\text{Ge}_{0.3}$  alloy.

parameters, and this variation has been investigated and displayed for different cases. Table 2 gives the physical parameters of the investigated materials used in the calculation. We also present the results of a rigorous calculation of  $ZT$  for the sake of comparison.

In figure 2, the results of calculations for  $\text{Bi}_2\text{Te}_3$  are displayed for temperature range (200–300 K) in steps of 50 K. Figure 2a shows  $ZT$  and figure 2b shows  $m$ . Temperatures selected for the purpose are based on the optimum performance range of the material. All three curves for different temperatures show that the variation of  $m$  approaches maximum sharply and then decreases slowly with increase in the carrier concentration. The  $ZT$  plots show somewhat similar variation. At temperatures beyond the maximum the  $m$  vs.  $n$  curves have a tendency to approach almost constant value. The onset of this region may mark the ideal operating temperature for material under consideration. For a particular temperature

**Table 2.** Physical parameters of Bi<sub>2</sub>Te<sub>3</sub>, PbTe and Si<sub>0.7</sub>Ge<sub>0.3</sub> at room temperature used in the calculations.

	$E_g$ (eV)	$m_d^*/m_0$	$C_{11}$ (Nm <sup>-2</sup> ) × 10 <sup>11</sup>	$\xi_D$ (eV)	$\lambda_L$ (W m <sup>-1</sup> K <sup>-1</sup> )	$N_V$
Bi <sub>2</sub> Te <sub>3</sub>	0.15	0.16	0.19	6.3	1.6	6
PbTe	0.32	0.20	1.39	24	2.0	4
Si <sub>0.7</sub> Ge <sub>0.3</sub>	0.97	0.9	1.55	12.8	7.6	6

$T = 250$  K the maximum value of  $ZT = 0.65$  and at that point carrier density  $n = 7.5 * 10^{18}$  cm<sup>-3</sup> and the value of  $m = -105$   $\mu$ V/K. Figures 3a and 3b display the same results in a 3D visualization. One can see that  $ZT$  plot acquires a peak, whereas the slope  $m$  shows a plateau and the onset of the plateau marks the optimal value of  $m$ .

Figures 4a and 4b display similar results for PbTe, the temperature range being 400–600 K. For  $T = 600$  K the slope  $m$  approaches a constant value. At  $T = 500$  K,  $ZT = 0.43$ ,  $n = 12 * 10^{18}$  cm<sup>-3</sup>, and slope  $m = -98$   $\mu$ V/K.

The results of calculation for Si<sub>0.7</sub>Ge<sub>0.3</sub> are displayed in figures 5a and 5b. The large energy gap of the alloy makes it useful at higher temperatures; hence the temperature range selected for this material is 1000–1400 K. The variation of  $m$  shows a similar nature as that of  $ZT$  when both are plotted against carrier density. One may conclude that  $m$  rises sharply with  $n$ , and acquires a maximum value. It then drops slowly with further rise of  $n$ . The value of  $n$  that gives the highest  $m$  is the optimum concentration for that temperature. The  $m$  is found in the range from  $-90$  to  $-105$  for best operating temperatures for all three materials under consideration, which is close to the value of slope [10],  $m$  approaches  $(k_B/e) = -86$   $\mu$ V/K. It is found that maximum of  $ZT$  and maximum of  $m$  shift towards left as  $T$  decreases. For fixed  $T$ , variation with  $n$  is almost identical in both the schemes. As regards the optimal values of  $T$  and  $n$ , the  $ZT$  plots are marked by peaks, whereas the slope  $m$  plots are marked by the onset of plateau region.

## Acknowledgement

Authors are thankful to M D Tiwari and Hari Prakash for their interest and support. MNT thanks Suneet Dwivedi and Anurag Baghel for suggestions and support.

## References

- [1] A F Ioffe, *Semiconductor thermoelements and thermoelectric cooling* (Infosearch, London, 1957) p. 53
- [2] H J Goldsmid, *Applications of thermoelectricity* (Methuen Monograph, London, 1960)
- [3] H J Goldsmid, *Electronic refrigeration* (Pion Ltd., London, 1986) p. 58
- [4] D M Rowe and C M Bhandari, *Modern thermoelectrics* (Holt Saunders Ltd., London, 1983)

*Material parameters for thermoelectric performance*

- [5] C M Bhandari, *CRC handbook of thermoelectrics* edited by D M Rowe (CRC, Boca Raton, Florida, 1995) vol. 27, ch. 4
- [6] H J Hrostowski, *Semiconductors* edited by N B Hannay (Reinhold Publishing Corporation, New York, 1959) p. 445
- [7] J R Drabble and H J Goldsmid, *Thermal conduction in semiconductors* (Pergamon Press, Oxford, 1961)
- [8] C M Bhandari and D M Rowe, *Thermal conduction in semiconductors* (Wiley Eastern Ltd., New Delhi, 1988)
- [9] D M Rowe and V S Shukla, *J. Appl. Phys.* **52**, 7421 (1981)
- [10] D M Rowe and Gao Min, *J. Mater. Sci. Lett.* **14**, 617 (1995)
- [11] C M Bhandari and D M Rowe, *Indian J. Pure Appl. Phys.* **34**, 579 (1996)
- [12] C M Bhandari, *Indian J. Pure Appl. Phys.* **37**, 434 (1999)
- [13] Y I Ravich, B A Efimova and V I Tamarchenko, *Phys. Status Solidi* **B43**, 11 (1971)
- [14] M N Tripathi and C M Bhandari, *J. Phys. C: Condens. Matter* **15**, 5359 (2003)
- [15] I A Smirnov and Y I Ravich, *Sov. Phys.- Semiconductors* **1**, 739 (1967)
- [16] D M Rowe and C M Bhandari, *J. Phys.* **D18**, 873 (1985)
- [17] M P Singh and C M Bhandari, *Solid State Commun.* **127**, 649 (2003)
- [18] R W Ure Jr., *Energy conversion* **12**, 45 (1972)
- [19] J O Sofo and G D Mahan, *Phys. Rev.* **B49**, 4565 (1994)